Electronic Supplementary Material (ESI) for Chemical Communications
This journal is © The Royal Society of Chemistry 2011

Electronic Supplementary Information

A polyoxometalate-based single-molecule magnet with an $S = 21/2$ ground state

Xikui Fang, Paul Kögerler, Manfred Speldrich, Helmut Schilder and Marshall Luban

Ames Laboratory, US DOE and Department of Physics and Astronomy, Iowa State University, Ames, IA 50011
Institute of Inorganic Chemistry, RWTH Aachen University, D-52074 Aachen, Germany

Page

This journal is © The Royal Society of Chemistry 2011

Synthesis of 2a: A sample of $[Mn^{III}_8Mn^{IV}_4O_{12}(CH_3COO)_{16}(H_2O)_4]\cdot 4H_2O\cdot 2CH_3COOH$ (0.15 g, 0.073 mmol) was suspended in H_2O (20 mL). Solid $Na_{12}[\alpha\text{-}P_2W_{15}O_{56}]\cdot 18H_2O$ (0.5 g, 0.12 mmol) was added to the mixture in small portions over a period of 10 min with vigorous stirring. After stirring for 0.5 hr at room temperature, the mixture was heated to 80 °C for another 1.5 hr and hot filtered. Solid NaCl (0.6 g) was then added to the filtrate. Slow evaporation of the solution first produced dark red crystals of **2a** (stacked plates) in about 2–3 weeks, with a yield of 70 mg (12.6 % based on W). If the solution was allowed for further evaporation, the Finke-type sandwich complex, $Na_{16}[(\alpha\text{-}P_2W_{15}O_{56})_2Mn_4(H_2O)_2]\cdot xH_2O$ (**3a**), precipitated as prismatic crystals.[1,2] Due to notable differences in the solubility and crystal morphology, it was possible to isolate the pure phase of **2a** before the first crystals of **3a** appeared.

Crystal samples of **2a** had an exceptionally high content of solvent water, approximately 68 H_2O per molecule (12.8%) based on crystal analysis (the actual number of water molecules might be even higher given the disorder associated with loosely bound solvent molecules); they easily release their lattice water upon removal from the mother solution and developed crack within a minute. Consequently, TG/DTA results (Fig. S1) showed a much lower water content (7.9%). In contrast, crystals of **3a** were considerably more resistant to water loss and retained crystallinity even after hours of exposure to air. Elemental analysis, calcd. for $Na_{14}[(\alpha\text{-}P_2W_{15}O_{56})_2Mn^{III}_6Mn^{IV}O_6(H_2O)_6]\cdot 32H_2O$: Mn 4.31, P 1.39, W 61.8, Na, 3.61 %. Found: Mn 4.46, P 1.22, W 58.4, Na 3.39 %. Selected IR bands for **2a** (KBr pellet): 1085(s), 1061(w, sh), 1009(w), 946(s), 915(m), 879(m), 813(vs, br), 722(m), 584(w), 563(w), 521(m). The ^{31}P NMR spectrum of **2a** (in D_2O, Fig. S2) indicates that the solid state structure is retained in solution. It exhibits only one broad peak at −11.7 ppm ($\Delta\nu_{1/2}$ = 125 Hz), which is attributed to the two distal phosphorus atoms (P2). The signal for the two proximal phosphorus atoms (P1) is too broadened for detection, due to their close proximity to the paramagnetic Mn centers.

(1) R. G. Finke, M. W. Droege and P. J. Domaille, *Inorg. Chem.*, 1987, **26**, 3886.
(2) C. J. Gómez-García, J. J. Borrás-Almenar, E. Coronado and L. Ouahab, *Inorg. Chem.*, 1994, **33**, 4016.

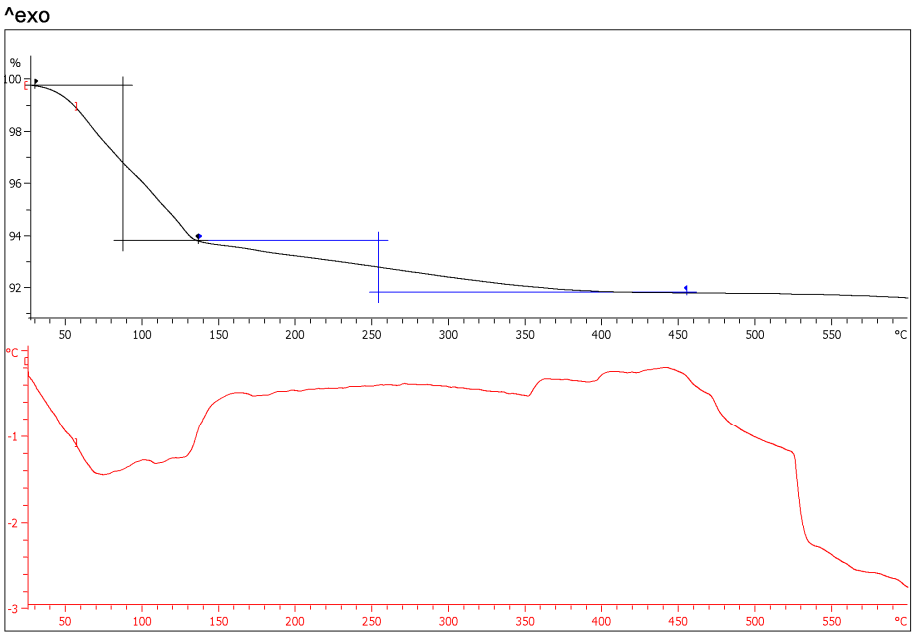

Fig. S1. TG and simultaneous DTA graphs of **2a** (10 K/min, 60 ml N_2/min).

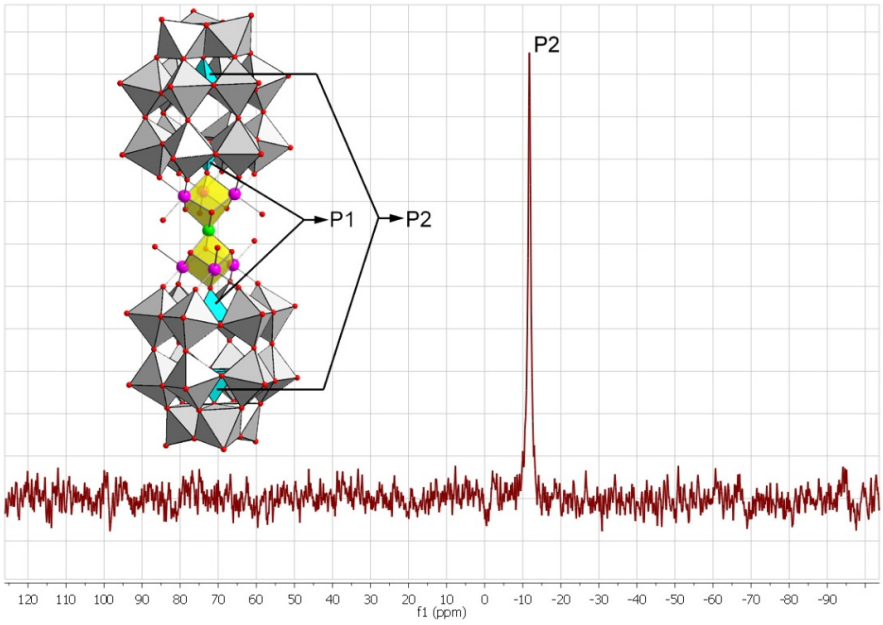

Fig. S2. ^{31}P NMR spectrum of **2a** (6.62 mmol L^{-1} in D_2O, referenced to 85% H_3PO_4).

Instruments and physical measurements: Infrared spectra (KBr pellets) were collected with a Brüker Tensor 27 instrument. Elemental analyses are performed by Columbia Analytical Service, Tucson, AZ. The dc susceptibilities of **2a** were determined by SQUID magnetometry (Quantum Design MPMS-5XL) for T = 1.8 – 300 K at an applied field 0.1 T and for T = 1.8 – 6.0 K for different applied fields (B = 2 – 5 T). The data were corrected for the sample holder (PTFE capsules) and diamagnetic/TIP contributions ($\chi_{dia/TIP}$(**2a**) = -7.22×10^{-8} m^3mol^{-1}). Initial values for the real ligand field parameters B^k_q (Wybourne notation)were chosen from reference 3.

(3) (*a*) K. B. Gorller-Walrand C., in *Handbook on the Physics and Chemistry of Rare Earths*, Vol. 23 (Eds.: J. K. A. Gschneidner, L. Eyring), Elsevier, Amsterdam, 1996; (*b*) B. G. Wybourne, *Spectroscopic Properties of Rare Earths*, Wiley, New York, 1965.

X-ray crystallographic structure determination: Suitable crystals were coated with Paratone-N oil, suspended on a small fiber loop, and placed in a cooled nitrogen stream at 173(2) K on a Brüker SMART 1000 CCD sealed-tube diffractometer with graphite-monochromated Mo Kα (0.71073 Å) radiation. A sphere of data was measured using a series of combinations of ϕ and ω scans with 10 s frame exposures and 0.3° frame widths. Data collection, indexing, and initial cell refinements were all handled using SMART software.[4] Frame integration and final cell refinements were carried out using SAINT software.[5] The SADABS program was used to carry out absorption corrections.[6] The structure was solved using Direct Methods and difference Fourier techniques (SHELXTL, V6.12).[7] All metal atoms (W and Mn) were refined anisotropically; the rest were isotropically refined. Scattering factors and anomalous dispersion corrections were taken from the International Tables for X-ray Crystallography.[8] Structure solution, refinement and generation of the crystallographic information file were performed by using SHELXTL, V6.12 software.[7] Not all of the counterions (Na^+) and the lattice water molecules could be located due to disorder. Therefore, thermogravimetric and elemental analyses were used to determine the number of water molecules and countercations, instead.

(4) SMART Version 5.628, 2003, Brüker AXS, Inc., Analytical X-ray Systems, 5465 East Cheryl Parkway, Madison WI 53711-5373.
(5) SAINT Version 6.36A, 2002, Brüker AXS, Inc., Analytical X-ray Systems, 5465 East Cheryl Parkway, Madison WI 53711-5373.
(6) SADABS Version 2.08, 2003, George Sheldrick, University of Göttingen.
(7) SHELXTL 6.12, 2002, Brüker AXS, Inc., Analytical X-ray Systems, 5465 East Cheryl Parkway, Madison WI 53711-5373.
(8) Wilson, A. J. C., Ed.; *International Tables for X-ray Crystallography, Volume III.* Academic Publishers: Dordrecht, 1992, Tables 6.61.1.4 (pp. 500–502) and 4.2.6.8 (pp. 219–222).

Bond valence sum calculations: For determination of the oxidation states of metal centers and the protonation states of oxygen sites, bond valence sum (BVS) calculations were carried out using the method of I. D. Brown (See, I. D. Brown and D. Altermatt, *Acta Crystallogr. Sect. B*, 1985, **41**, 244). The R_0 values were taken from the literature for calculations performed on Mn[9] and O[9–11] sites.

(9) W. Liu and H. H. Thorp, *Inorg. Chem.*, 1993, **32**, 4102.
(10) P. L. Roulhac and G. J. Palenik, *Inorg. Chem.*, 2003, **42**, 118.
(11) N. E. Brese and M. O'Keeffe, *Acta Crystallogr. Sect. B*, 1991, **47**, 192.

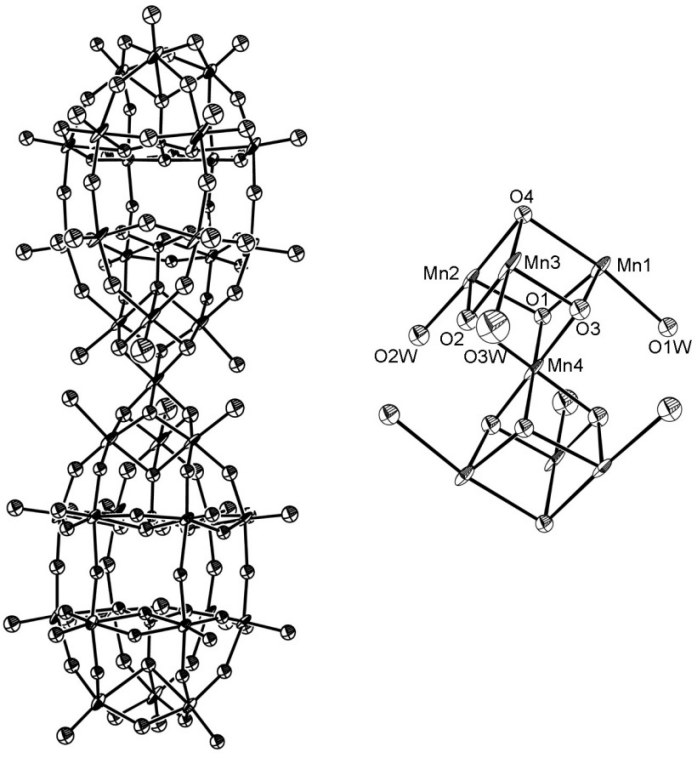

	BVS[6]		
	Mn(II)	Mn(III)	Mn(IV)
Mn1	3.23	**2.95**	3.10
Mn2	3.25	**2.98**	3.12
Mn3	3.26	**2.98**	3.13
Mn4	4.06	3.71	**3.90**

Oxygen atoms	BVS[6—8]	Assigned Protonation levels
O1	1.79	**O**
O2	1.80	**O**
O3	1.84	**O**
O4	2.08	**O**
O1W	0.30	**H_2O**
O2W	0.29	**H_2O**
O3W	0.31	**H_2O**

Fig. S3. Bond valence sum (BVS) calculations for Mn centers and oxygen sites of the Mn_7 core in **2a**. The assigned oxidation states and protonation levels are highlighted in bold and shaded.

Magnetic simulations: An accurate magnetochemical interpretation of the $\{Mn^{III}_6Mn^{IV}\}$ spin polytope in **2a** relies on modeling all relevant single-ion effects (interelectronic repulsion, H_{ee}; spin–orbit coupling, H_{so}; ligand field (lf) effects, H_{lf}; and the applied magnetic field, H_{mag}) as well as Heisenberg-type exchange coupling (H_{ex}), yielding the Hamiltonian $\hat{H} = \hat{H}_{ee} + \hat{H}_{lf} + \hat{H}_{so} + \hat{H}_{mag} + \hat{H}_{ex}$. The influence of the tetragonal ligand field with reference to the rotation axis for the angular part of the wave function is described by

$$\hat{H}_{lf}^{tet} = B_0^2 \sum_{i=1}^{N} C_0^2(i) + B_0^4 \sum_{i=1}^{N} C_0^4(i) + B_4^4 \sum_{i=1}^{N} \left(C_4^4(i) + C_{-4}^4(i)\right)$$

The full Hamiltonian is defined as

$$\begin{aligned}\hat{H} \;=\; & \underbrace{\sum_{i=1}^{N}\left[-\frac{\hbar^2}{2m_e}\nabla_i^2 + V(r_i)\right]}_{\hat{H}^{(0)}} + \underbrace{\sum_{i>j}^{N}\frac{e^2}{r_{ij}}}_{\hat{H}_{ee}} + \underbrace{\sum_{i=1}^{N}\zeta(r_i)\,\kappa\;\hat{\boldsymbol{l}}_i\cdot\;\hat{\boldsymbol{s}}_i}_{\hat{H}_{so}} + \\ & \underbrace{\sum_{i=1}^{N}\sum_{k=0}^{\infty}\left\{B_0^k C_0^k(i) + \sum_{q=2}^{k}\left[B_q^k\left(C_{-q}^k(i) + (-1)^q C_q^k(i)\right)\right]\right\}}_{\hat{H}_{LF}} + \\ & \underbrace{\sum_{i=1}^{N}\mu_B(\kappa\;\hat{\boldsymbol{l}}_i + 2\;\hat{\boldsymbol{s}}_i)\cdot\;\boldsymbol{B}}_{\hat{H}_{mag}}\end{aligned}$$

and augmented by the Heisenberg exchange Hamilton (see above). The Hamiltonian is implemented in the computational framework CONDON, which takes into account the full d manifolds, i.e. 210 for Mn^{III} ($3d^4$) and 120 for Mn^{IV} ($3d^3$), which are required to accurately describe the magnetic dipole orientation with respect to the local symmetry elements.

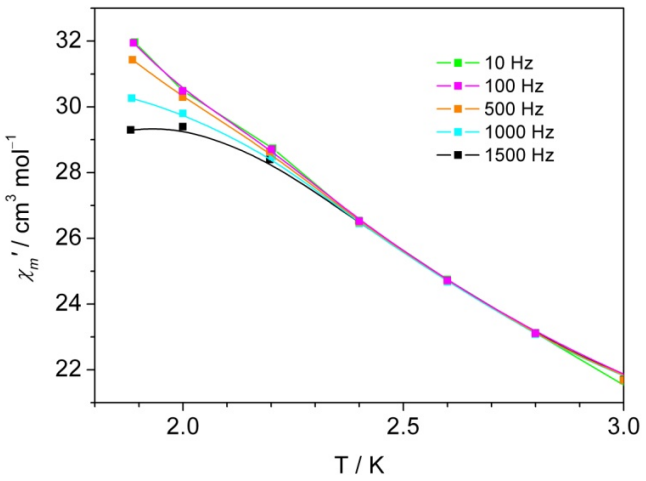

Fig. S4. In-phase ac susceptibility data (χ'_m) for **2a**.